SUPPLEMENTAL INFORMATION

Supplemental information includes seven figures, two tables, and one movie.

Supplemental Figures

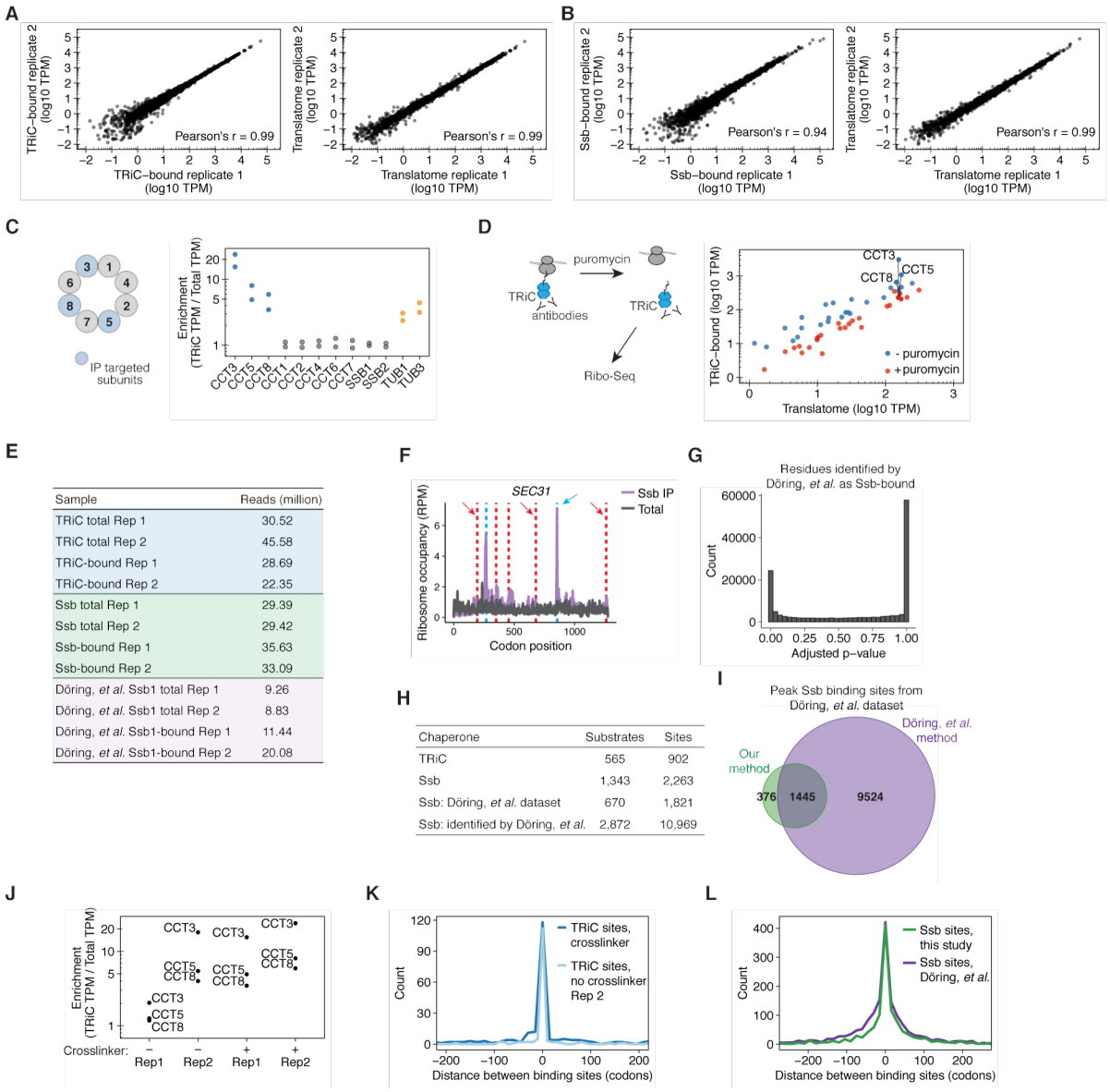

Sample	Reads (million)
TRiC total Rep 1	30.52
TRiC total Rep 2	45.58
TRiC-bound Rep 1	28.69
TRiC-bound Rep 2	22.35
Ssb total Rep 1	29.39
Ssb total Rep 2	29.42
Ssb-bound Rep 1	35.63
Ssb-bound Rep 2	33.09
Döring, *et al.* Ssb1 total Rep 1	9.26
Döring, *et al.* Ssb1 total Rep 2	8.83
Döring, *et al.* Ssb1-bound Rep 1	11.44
Döring, *et al.* Ssb1-bound Rep 2	20.08

Chaperone	Substrates	Sites
TRiC	565	902
Ssb	1,343	2,263
Ssb: Döring, *et al.* dataset	670	1,821
Ssb: identified by Döring, *et al.*	2,872	10,969

Figure S1. Cotranslational enrichment of TRiC and Ssb on ribosome-nascent chains, Related to Figure 1

(A) Gene enrichment from total and TRiC-bound translatomes from two biological replicates.

(B) Gene enrichment from total and Ssb-bound translatomes from two biological replicates.

(C) TRiC enrichment of all TRiC subunits, including the subunits targeted by immunoprecipitation (*CCT3*, *CCT5*, and *CCT8*), as well as the Ssb subunits and the TRiC substrates *TUB1* and *TUB3*.

(D) TRiC enrichment of immunoprecipitation-targeted TRiC subunits and TRiC substrates that were enriched at the gene-level after performing lysis in the presence (red) or absence (blue) of puromycin treatment. Puromycin treatment dissociates the ribosome-protected mRNA from the TRiC-bound nascent

chain substrate (or the nascent chain of the TRiC subunit) that is targeted by immunoprecipitation antibodies.

(E) Sequencing coverage of our datasets compared to previous work. Also see Table S1.

(F) Ribosome occupancy profile of the total fraction (dark gray) and pulldown fraction (purple) for *SEC31* using the dataset from Döring, *et al*. Vertical lines represent peaks of Ssb enrichment identified by different analysis methods: 1) in blue, positions identified by our analysis and that of Döring, *et al.*, 2) in red, low-confidence peaks only identified by Döring, *et al*., particularly those marked with a red arrow.

(G) Histogram showing the adjusted p-values calculated using our analysis method for the 10,969 Ssb binding sites (147,226 total residues) identified by Döring, *et al*., showing that many of these residues do not have statistically significant Ssb enrichment.

(H) Number of substrates and peak binding sites identified in each dataset and depending on the type of analysis (i.e. our analysis strategy or that of Döring, *et al*. applied to the Döring, *et al*. dataset).

(I) Using the dataset from Döring, *et al*., our analysis strategy identifies fewer Ssb binding sites, but with substantial overlap with those identified by the analysis strategy employed by Döring, *et al*.

(J) Enrichment of TRiC subunits in libraries prepared with or without crosslinker. Addition of crosslinker during cell lysis improves reproducibility of immunoprecipitation efficiency.

(K) Crosslinker does not affect positional enrichment. Histogram showing the positional correlation of TRiC binding sites identified in crosslinked samples and the replicate 2 library that had no crosslinker added. The codon distance was calculated between the TRiC binding sites in the crosslinked samples to the nearest TRiC binding site identified in the sample without crosslinker (dark blue), as well as the converse in light blue (i.e. calculating the distance between sites identified in the library prepared without crosslinker to the nearest position identified in the crosslinked samples). n = 109 ORFs with 233 positions identified in the crosslinked samples and 154 positions identified in the sample without crosslinker.

(L) Comparison of Ssb datasets when using the same analysis strategy. Histogram showing the positional correlation of Ssb binding sites identified by this study as well as using our methodology on the previous Ssb dataset (Döring et al., 2017). The codon distance was calculated between the Ssb binding sites that we identify to the nearest Ssb binding site identified using our methodology on the previous Ssb dataset (Döring et al., 2017) (green), as well as the converse in purple (i.e. calculating the distance between sites identified by applying our methodology on the previous Ssb dataset (Döring et al., 2017) to the nearest position identified in our dataset). n = 547 ORFs with 1,187 positions identified in our dataset and 1,637 positions identified using our methodology on the previous Ssb dataset (Döring et al., 2017).

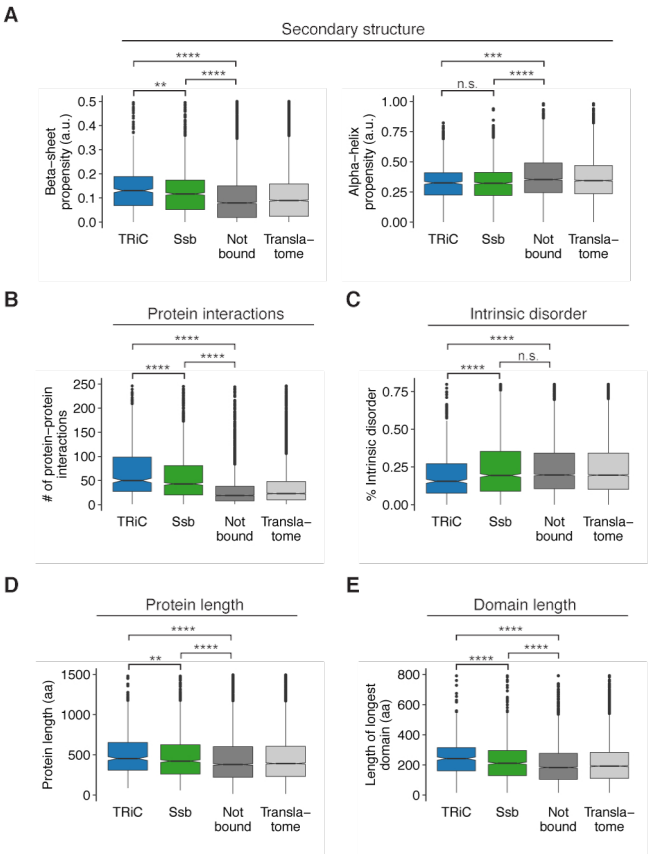

Figure S2. Properties of TRiC and Ssb nascent chain substrates, Related to Figure 1
(A – E) Intrinsic properties of TRiC (n = 565) and Ssb (n = 1,343) nascent chain substrates compared to the proteins not identified as substrates (n = 4,358) and to the translatome as a whole (n = 5,793). ****P < $1e^{-4}$, ***P < $1e^{-3}$, **P < 0.01, n.s. = not significant, Wilcoxon rank-sum test.

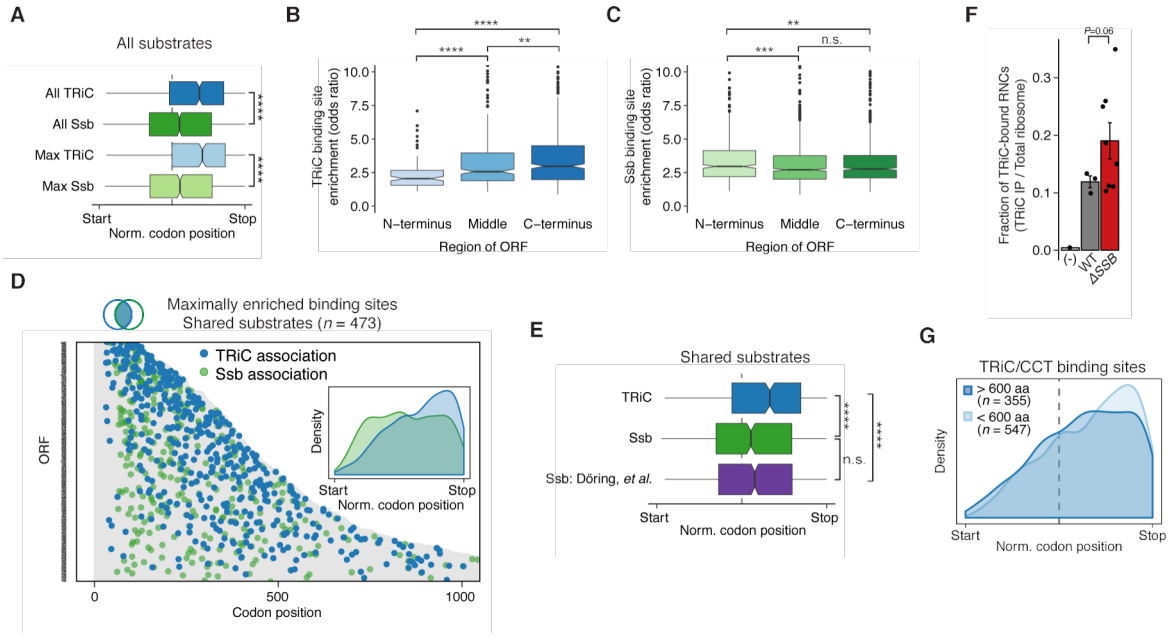

Figure S3. Distinct temporal dynamics define TRiC and Ssb recruitment, Related to Figure 2

(A) Positional distributions of all binding sites (n = 902 TRiC binding sites in 565 ORFs and 2,263 Ssb binding sites in 1,343 ORFs; $P = 4.9e^{-24}$, Wilcoxon rank-sum test), as well as maximally enriched binding sites (n = 565 TRiC binding sites and 1,343 Ssb binding sites; $P = 9.1e^{-19}$, Wilcoxon rank-sum test), after normalizing for protein length for all TRiC and Ssb substrates. Maximally enriched binding sites are defined as the one binding site in each transcript having the highest TRiC or Ssb enrichment (odds ratios), which were used to give each substrate equal weight.

(B – C) Enrichment of (B) TRiC and (C) Ssb relative to substrate transcript position. Identified binding sites in TRiC substrates (n = 565) and Ssb substrates (n = 1,343) were grouped into the N-terminal, middle, or C-terminal thirds of the transcript. $^{****}P < 1e^{-4}$, $^{***}P < 1e^{-3}$, $^{**}P < 0.01$, Wilcoxon rank-sum test.

(D) Heat map showing the position of peak enrichment of maximally enriched TRiC and Ssb positions in shared substrates (n = 473), with density distributions inset. ORFs are sorted by protein length and colored in gray. $P = 5.3e^{-10}$, Wilcoxon rank-sum test.

(E) Positional distributions of TRiC binding sites (blue, n = 535 sites), Ssb binding sites identified in this study (green, n = 809 sites), or Ssb binding sites identified by applying our methodology on the previous Ssb dataset (Döring et al., 2017) (purple, n = 1,087 sites), in substrates common to all three datasets (n = 297) after normalizing for protein length. $^{****}P < 1e^{-4}$, n.s. = not significant, Wilcoxon rank-sum test.

(F) Fraction of ^{35}S-labeled nascent chains bound by TRiC in wild-type (WT) or Δ*SSB* strains. $n \geq 3$ biological replicates with mean ± SEM. $P = 0.06$, Welch's t-test.

(G) Density distributions of TRiC binding sites based on protein size (substrates shorter or longer than 600 amino acid residues) after normalizing for protein length. $P = 0.04$, Wilcoxon rank-sum test.

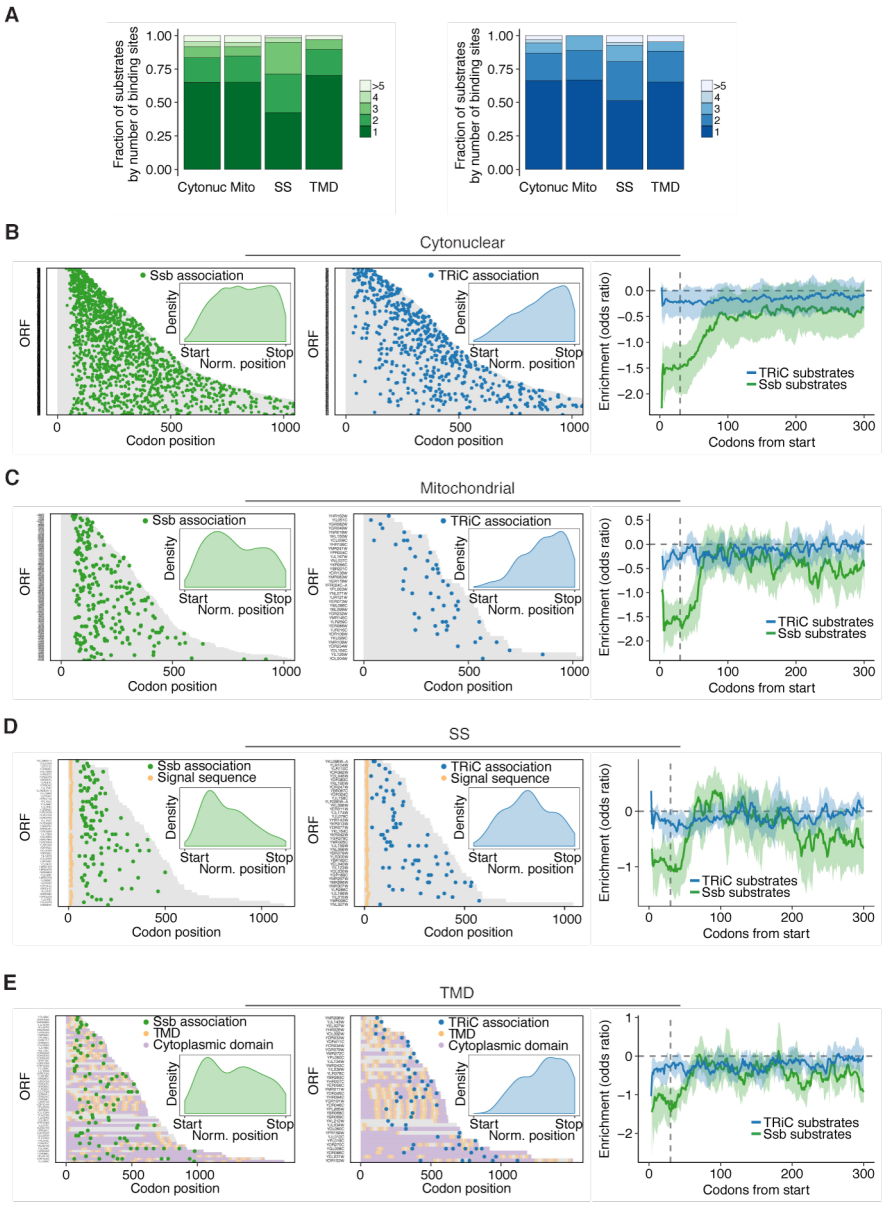

Figure S4. Substrate localization modulates chaperone association, Related to Figure 2

(A) Fraction of Ssb or TRiC substrates having the indicated number of binding sites for the indicated protein classes.

(B – E) Heat maps and density distributions showing the position of peak enrichment of all Ssb and TRiC binding sites in their respective sets of substrates classified as (B) cytoplasmic (1,600 Ssb sites in 944 ORFs; 613 TRiC sites in 387 ORFs), (C) mitochondrial (237 Ssb sites in 143 ORFs; 52 TRiC sites in 36 ORFs), (D) secretory proteins with a signal sequence (115 Ssb sites in 59 ORFs; 74 TRiC sites in 41 ORFs), or (E) secretory proteins with a transmembrane domain as the targeting signal (101 Ssb sites in 67 ORFs; 68 TRiC sites in 43 ORFs). ORFs are sorted by protein length and colored in gray, and the positions of indicated domains is also shown. Metagene analysis of TRiC and Ssb enrichment profiles is shown on the right. Lines represent the median enrichment and the shaded region is the interquartile range.

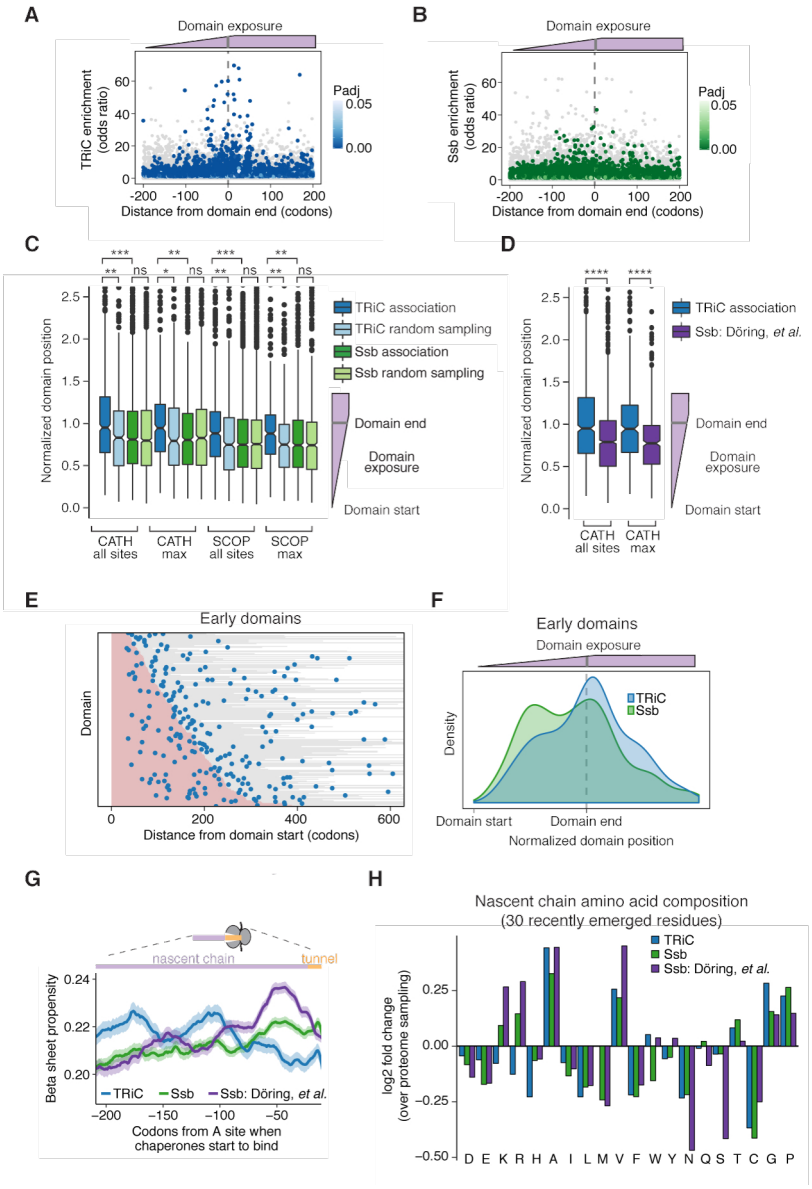

Figure S5. Structural and sequence elements dictate cotranslational chaperone recruitment, Related to Figure 3

(A – B) Enrichment of (A) TRiC or (B) Ssb in substrates aligned to the end of the nearest exposed protein domain, the last ~30 residues of which are in the ribosome tunnel. Each point represents a residue in the substrates of TRiC (n = 418) or Ssb (n = 904) with coloring indicating positions with statistically significant chaperone enrichment.

(C) Positional enrichment of all TRiC and Ssb binding events in reference to the nearest domain defined by either the CATH database (n = 683 TRiC sites in 418 ORFs, 1,585 Ssb sites in 904 ORFs) or SCOP database (n = 717 TRiC sites in 440 ORFs, 1,661 Ssb sites in 951 ORFs), or just the binding events where TRiC or Ssb is maximally enriched in each coding sequence. Domain length was normalized such that the domain start is at 0 and the domain end is at 1. Significance was determined by comparing to sets of randomly sampled positions from each substrate (see STAR Methods). ***$P < 1e^{-8}$, **$P < 1e^{-5}$, *$P < 1e^{-3}$, ns = not significant, Wilcoxon rank-sum test.

(D) As in (C) for TRiC binding events compared to the Ssb binding events that we identified using the previously published Ssb dataset (Döring et al., 2017) (n = 1,447 sites in 505 ORFs). ****$P < 1e^{-10}$, Wilcoxon rank-sum test.

(E – F) Heat map showing the position of peak enrichment of all TRiC binding sites in reference to the start of domains that are fully emerged early in translation, i.e. before ¾ of the protein is translated. The associated density distributions are shown in (F). n = 358 TRiC sites assigned to 249 domains in 216 ORFs, and 881 Ssb sites assigned to 610 domains in 520 ORFs. $P = 1.3e^{-8}$, Wilcoxon rank-sum test.

(G) Propensity of β sheet secondary structure in the nascent chain at the start of chaperone recruitment for the Ssb sites we identified using the previously published Ssb dataset (Döring et al., 2017) (purple, n = 1,821) as compared to the TRiC and Ssb sites from our datasets (as shown in Figures 3E and 3F). The line represents the mean β sheet propensity and the shaded region is the 95% bootstrapped confidence interval.

(H) Amino acid enrichment in the nascent chain at the sites of TRiC (n = 806) or Ssb (n = 2,220) recruitment as compared to the sites of Ssb recruitment we identified using the previously published Ssb dataset (Döring et al., 2017) (n = 1,776). Enrichment calculated based on the average amino acid composition of 10,000 randomly sampled sequences.

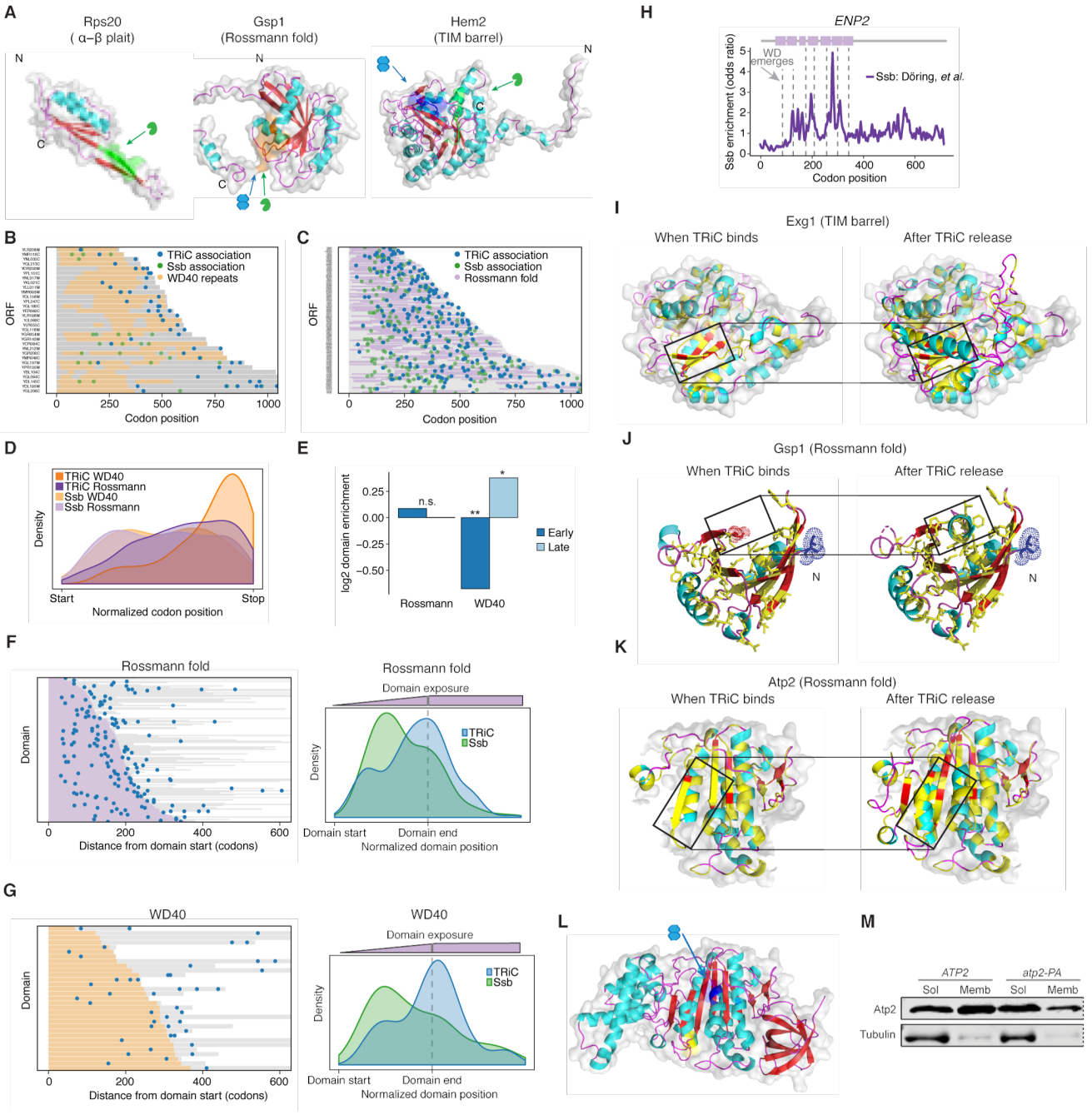

Figure S6. Linking chaperone recruitment to the structural landscape of domain-specific folding intermediates, Related to Figures 3, 4, and 5

(A) Examples of proteins having TRiC or Ssb enriched domains: Rps20 (PDB ID: 4U4R (Garreau de Loubresse et al., 2014)), Gsp1 (PDB ID: 3M1I (Koyama and Matsuura, 2010)), and Hem2 (PDB ID: 1H7N (Erskine et al., 2001)). Cartoon colored according to secondary structure. Colored surface positions indicate the sites of the nascent chain that just emerged when TRiC (blue), Ssb (green), or both (orange) chaperones bind.

(B – C) Heat map showing the position of peak enrichment of all TRiC and Ssb binding sites in TRiC substrates having (B) a WD40 domain (n = 31), or (C) a Rossmann fold (n = 139).

(D) Density distribution of TRiC and Ssb binding sites normalized by protein length, using the position of peak enrichment of all sites as in (B) and (C). $P = 4.0e^{-5}$ for the pairwise comparison of TRiC WD40 to TRiC Rossmann, Wilcoxon rank-sum test.

(E) Domain enrichment in TRiC substrates based on timing of binding. Substrates were grouped by having an early or late TRiC binding event, i.e. before or after ¾ of the protein is translated. $^{**}P = 0.002$, $^{*}P = 0.04$, n.s. = not significant.

(F – G) Heat map showing the position of peak enrichment of all TRiC binding sites (associated density plot also shows Ssb sites) in reference to the domain start of: (F) Rossmann folds (purple), $n = 176$ TRiC sites assigned to 126 domains in 105 ORFs, and 365 Ssb sites assigned to 264 domains in 226 ORFs; $P = 2.3e^{-5}$, Wilcoxon rank-sum test, or (G) WD40 domains (orange), $n = 52$ TRiC sites assigned to 31 domains in 30 ORFs, and 68 Ssb sites assigned to 47 domains in 39 ORFs; $P = 0.001$, Wilcoxon rank-sum test. Gray lines in the heat maps indicate the length of the protein beyond the domain end.

(H) Positional enrichment of Ssb in WD40 protein *ENP2* using the previously published Ssb dataset (Döring et al., 2017). Dashed gray lines indicate where the WD40 repeats emerge. Compare to Figure 4A.

(I) Structure of Exg1's TIM barrel domain (PDB ID: 1H4P (Taylor et al., 2004)) exposed from the ribosome at the point TRiC binds (left) as well as the complete domain after TRiC is released (right). Cartoon colored according to secondary structure, with hydrophobic residues in yellow, and surface representation of just the region exposed before TRiC binds. Box denotes the nascent chain that emerges just before TRiC binds consisting of a patch of hydrophobic β sheets that is buried by α helices after TRiC recruitment.

(J) As in (I) for Gsp1's Rossmann fold domain (PDB ID: 3M1I (Koyama and Matsuura, 2010)), with hydrophobic residues in stick representation. A different orientation of Figure 5D.

(K) As in (I) for Atp2's Rossmann fold domain (PDB ID: 2XOK (Stock et al., 1999)).

(L) Structure of Atp2 (PDB ID: 2XOK (Stock et al., 1999)). Cartoon colored according to secondary structure. Positions colored blue indicate the nascent chain that has just emerged when TRiC binds. Positions colored in yellow are the proline residues in the ribosome active site when TRiC binds that are mutated in *atp2-P353,355A* cells.

(M) Subcellular fractionation into soluble and membrane fractions of cells harboring WT *ATP2* or mutant *atp2-P353,355A*, and subjected to western blot using the indicated antibodies. $n = 3$ biological replicates with a representative example shown and superfluous lanes cropped at dotted line.

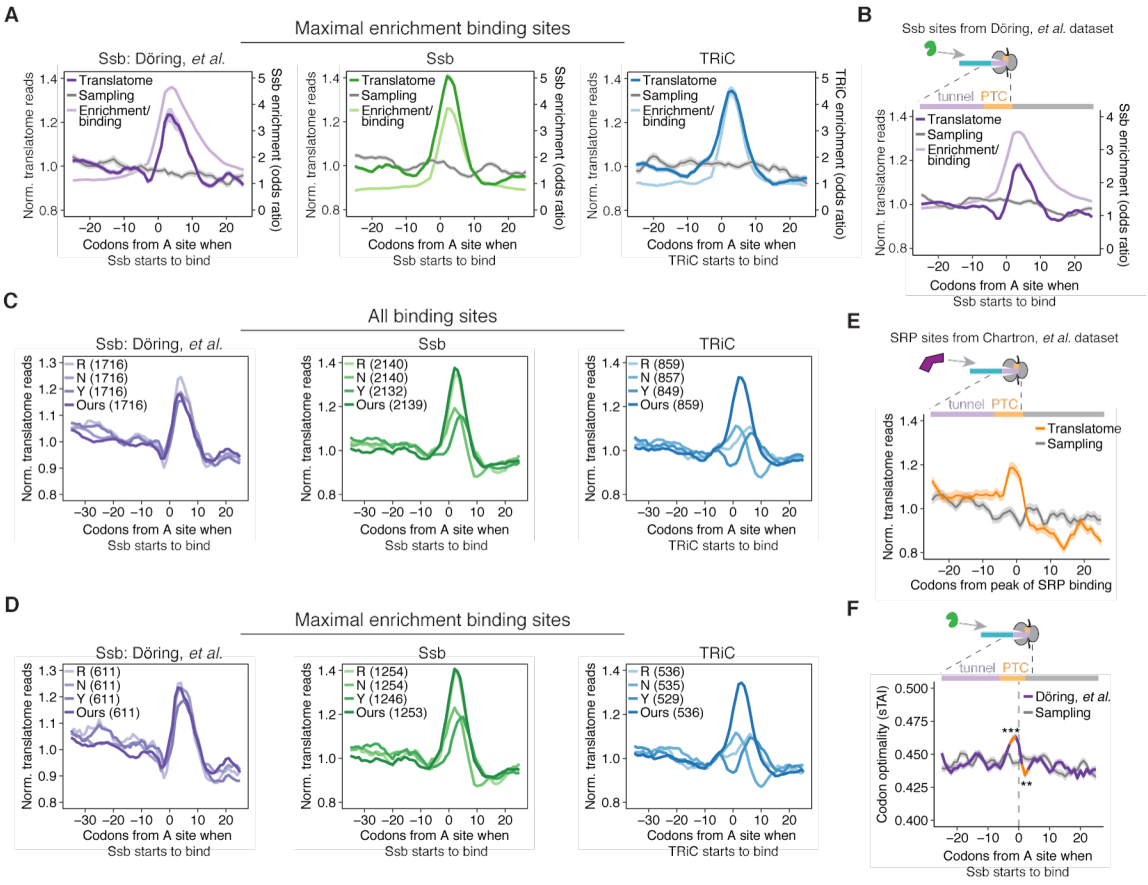

Figure S7. Chaperone association is coordinated with changes in elongation rate, Related to Figure 6

(A) Metagene analysis of translation kinetics. Dark colored lines represent the mean ribosome occupancy of the translatome, and lightly colored lines represent the mean chaperone enrichment (odds ratio), centered around the peptidyl transferase center (PTC) at the start of chaperone binding at the sites of highest chaperone enrichment in each substrate (to give each gene equal weight) for: 1) Ssb sites that we identified using the previously published Ssb dataset (Döring et al., 2017) (purple, n = 670), 2) Ssb sites identified in our dataset (green, n = 1,343), and 3) TRiC sites (blue, n = 565). Gray lines represent the mean ribosome occupancy of the translatome at an equivalent number of randomly sampled positions in the respective set of substrates. Shaded regions are the 95% bootstrapped confidence interval.

(B) Metagene analysis of translation kinetics at Ssb binding sites we identified using the previously published Ssb dataset (Döring et al., 2017). Dark purple line represents the mean ribosome occupancy of the translatome, and light purple line represents the mean Ssb enrichment (odds ratio), centered around the PTC at the start of Ssb binding sites (n = 1,821). Gray line represents the mean ribosome occupancy at an equivalent number of randomly sampled positions in the substrate set. Shaded regions are the 95% bootstrapped confidence interval.

(C – D) Metagene analysis of translation kinetics with lines representing the mean ribosome occupancy of the translatome centered around the PTC at the start of chaperone binding using previously published ribosome profiling datasets (R: (Radhakrishnan et al., 2016), N: (Nedialkova and Leidel, 2015), Y: (Young et al., 2015)) for (C) all chaperone binding sites, and (D) the site of highest chaperone enrichment in each substrate. The number of binding sites (n) that are analyzed is shown in parentheses for each dataset, which varies based on dataset coverage.

(E) Metagene analysis of translation kinetics at SRP binding sites identified previously (Chartron et al., 2016). Orange line represents the mean ribosome occupancy of the translatome centered around the PTC of the pronounced SRP binding sites (n = 228). Gray line represents the mean ribosome occupancy at an equivalent number of randomly sampled positions in the substrate set. Shaded regions are the 95% bootstrapped confidence interval.

(F) Metagene analysis of codon optimality at Ssb binding sites we identified using the previously published Ssb dataset (Döring et al., 2017). Purple line represents the mean codon optimality centered around the PTC at the start of Ssb binding sites (n = 1,821). Codon optimality was measured using the species-specific tRNA adaptation index (sTAI) (Sabi and Tuller, 2014). Gray line represents the codon optimality at an equivalent number of randomly sampled positions in the substrate set. Shaded regions are the 95% bootstrapped confidence interval. Significance was tested by comparing the distribution of codon optimality in the 3 residue window before and after the start of chaperone binding to the equivalent window around the randomly sampled positions. ***$P = 5.8e^{-4}$, **$P = 0.01$, Wilcoxon rank-sum test.

Supplemental Tables

Sample	Reads (million)	Reference
TRiC-bound Rep 1	28.69	This study; GEO: GSE114882
TRiC-bound Rep 2	22.35	This study; GEO: GSE114882
TRiC total Rep 1	30.52	This study; GEO: GSE114882
TRiC total Rep 2	45.58	This study; GEO: GSE114882
TRiC-bound puromycin Rep 1	8.96	This study; GEO: GSE114882
TRiC-bound puromycin Rep 2	0.87	This study; GEO: GSE114882
TRiC total puromycin Rep 1	7.86	This study; GEO: GSE114882
TRiC total puromycin Rep 2	11.60	This study; GEO: GSE114882
Ssb-bound Rep 1	35.63	This study; GEO: GSE114882
Ssb-bound Rep 2	33.09	This study; GEO: GSE114882
Ssb total Rep 1	29.39	This study; GEO: GSE114882
Ssb total Rep 2	29.42	This study; GEO: GSE114882
Ssb-bound puromycin Rep 1	10.59	This study; GEO: GSE114882
Ssb-bound puromycin Rep 2	20.74	This study; GEO: GSE114882
Ssb total puromycin Rep 1	31.24	This study; GEO: GSE114882
Ssb total puromycin Rep 2	34.86	This study; GEO: GSE114882
atp2 mutant TRiC-bound Rep 1	36.39	This study; GEO: GSE114882
atp2 mutant TRiC-bound Rep 2	45.09	This study; GEO: GSE114882
atp2 mutant TRiC total Rep 1	92.74	This study; GEO: GSE114882
atp2 mutant TRiC total Rep 2	130.70	This study; GEO: GSE114882
WT translatome no chx Rep 1	58.24	This study; GEO: GSE114882
WT translatome no chx Rep 2	48.21	This study; GEO: GSE114882
WT Ssb1-GFP translatome, Rep 1	9.26	(Döring et al., 2017); GEO: GSE93830
WT Ssb1-GFP translatome, Rep 2	8.83	(Döring et al., 2017); GEO: GSE93830
WT Ssb1 interactome, Rep 1	11.44	(Döring et al., 2017); GEO: GSE93830
WT Ssb1 interactome, Rep 2	20.08	(Döring et al., 2017); GEO: GSE93830
Wild-Type Profiling	54.11	(Radhakrishnan et al., 2016); GEO: GSE81269
Wild-Type Profiling (Replicate)	16.03	(Radhakrishnan et al., 2016); GEO: GSE81269
WT_ribo_YPD_rep1	15.06	(Nedialkova and Leidel, 2015); GEO: GSE67387
WT_ribo_YPD_rep2	13.34	(Nedialkova and Leidel, 2015); GEO: GSE67387
WT_ribo_YPD_rep3	13.16	(Nedialkova and Leidel, 2015); GEO: GSE67387
Wild-type	27.38	(Young et al., 2015); GEO: GSE69414

Table S1. Coverage of datasets analyzed in this study, Related to Figure 1
Indicated numbers of ribosome reads are the reads that mapped to coding sequences after removal of fragment lengths that did not show three nucleotide periodicity. Data are accessible at the NCBI GEO database (Edgar et al., 2002) using the indicated accession numbers.